Automatic Image Matching for Space Intersection of Spherical Panorama Images

Pin-Yun Chen[1], Yi-Hsing Tseng[2], Kuan-Ying Lin[3]
National Cheng Kung University, No.1, Daxue Rd., East Dist., Tainan City 701, Taiwan (R.O.C.)
Email: pinyunchen@gmail.com[1], tseng@mail.ncku.edu.tw[2] , azsxd2014@gmail.com[3]

KEY WORDS: Close-range Photogrammetry, Mobile Mapping System, Object Space Matching

ABSTRACT: People are paying more attention to the use of Spherical Panorama Images (SPIs) for its main advantage of wide field of view (FOV). Provide accurate location and orientation can enhance more metric application using SPIs. While the exterior orientation parameters (EOPs) of image stations are known, the coordinates of interested points can be determined by space intersection of multiple SPIs. In this study, a special platform called portable panoramic image mapping system (PPIMS) is used to obtain SPIs, and applied for photogrammetric mapping. This system equips with eight single lens cameras and one GNSS receiver, capturing surrounding information simultaneously. The images captured with PPIMS are combined to be a SPI, and then used for mapping application instead of using original images. The EOPs of image stations can be calculated by the network adjustment with multiple SPIs. No matter in solving image station EOPs or space intersection process, conjugate points selection among overlapped images is a necessary task. Image matching is considered as an approach to obtain conjugate points much more efficient than manual measurement. In this study, an area-based image matching strategy for automatic conjugate point detection and point coordinate determination with multiple SPIs is proposed. The Sum of Normalized Cross-Correlation (SNCC) and Yet Another Reconstruction Dataprogram (YARD) index are used to check the similarity between images. To decrease the influence caused by scale variations and different FOV between images, the concept of matching in the object space is applied to enhance the matching accuracy. This research shows the feasibility of spatial positioning of interested points with PPIMS SPIs in cm level accuracy. The proposed image matching strategy with PPIMS SPIs is applied and validated. The problem of scale variations and different FOV which causes problem in matching with original images can be improved by object space matching.

1. INTRODUCTION

Close-range photogrammetry (CRP) has been inspired to be an efficient mapping method as mobile mapping technology is developed. A new concept of CRP is proposed using panoramic images. With wide field of view (FOV) in single image with high resolution, surrounding information can be recorded in detail by taking only a few panoramas.

The portable panoramic image mapping system (PPIMS) is developed to capture panoramas with 8 single lens cameras, obtaining the position of image station with a GNSS receiver. Eight images captured by PPIMS simultaneously can formulate a spherical panorama image (SPI), and then used for photogrammetric mapping instead of using original images. Under this circumstance, one SPI is associated with only one set of exterior orientation parameters (EOPs). The mapping theory of PPIMS has been developed in recent years, Wang (2012) proposed a strategy for PPIMS system calibration to get the precise relationship between cameras, and the PPIMS SPI

formulation algorithm which maintains the geometric relationship between cameras was proposed. A bundle adjustment algorithm was proposed to solve EOPs of multi-station SPIs (Tsai, 2012; Lin, 2014), then object point position can be determined by the space intersection of panoramic image point observations.

Conjugation point measurement is a necessary step in CRP mapping process. Obtaining conjugate points of image sequences by image matching is believed to be much more efficient than manual measurement. Area-based image matching is a widely used technique, using the gray value of images to determine the similarity between images through the calculation with matching index, such as cross correlation or least squares correlation techniques (Gruen, 1985). Generally, the matching approach is applied on image space. However, the factors of scale variations, different FOV and object occlusion may result in incorrect matching points. The concept of matching in object space is proposed (Paparoditis et al., 2000) by adjusting the image scale and perspective through image resampling.

In this study, the first objective aims to implement photogrammetric mapping using PPIMS SPIs, apply space intersection to determine the coordinates of interest points. The second one focus on developing a suitable strategy for conjugate point matching among overlapped SPIs using area-based object space matching.

2. Spherical Panorama Image of PPIMS

PPIMS is designed for rapid acquisition of spatial data, and can be used in forest areas, disaster areas, or some locations that vehicle-based mobile mapping system is not allowed to enter. As shown in Figure 1(a), PPIMS has a platform that can mount eight single-lens cameras and one GNSS receiver. Eight cameras can capture images simultaneously by a trigger, and the GNSS receiver is fixed on the top for image station positioning. Three types of coordinate systems are included in the geometry of PPIMS: Camera Frame (C-Frame), Body Frame (B-Frame), and the Mapping Frame (M-Frame). Each camera has its own frame. The B-Frame is the coordinate system composed of PPIMS platform, the origin of B-Frame is set at the reference point of GNSS receiver. Figure 1(b) shows the relationship among these coordinate systems.

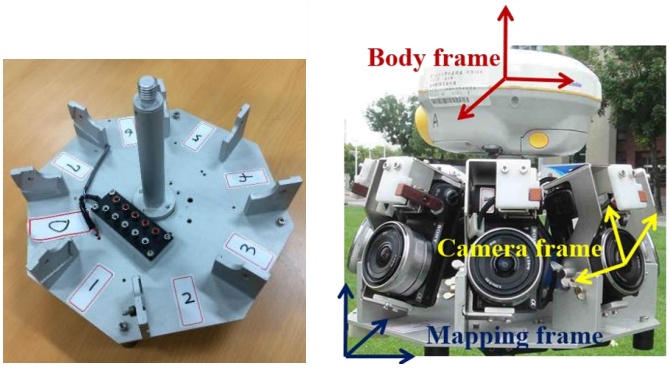

Figure 1 (a) Platform of PPIMS; (b) Coordinate systems in PPIMS geometry.

Before PPIMS is applied for photometric application, the interior orientation of eight cameras and the relative orientation between each camera and SPI center need to be calibrated. The relative orientation between each camera and SPI center include two parts: lever-arm offset and the rotation matrix which is formulated by boresight angle.

The idea of this study is to combine eight images captured at the same time to be a complete SPI. This kind of image is good for visualization and feasible for ray intersection. The following section describes how to generate a SPI with

eight images. Figure 2(a) shows the angular coordinate and pixel coordinate of PPIMS SPI. The center of PPIMS SPI is set at the origin of the B-Frame, and the SPI is formed by a spherical coordinate system. All object points are assumed to be at the same distance (R_{SPI}) from SPI center. Each pixel on the SPI can be described by the SPI radius (R_{SPI}), horizontal angle (α), and the zenith angle (ρ). Considering the resolution of original images, the SPI pixel angular resolution is set to $1'$. So that α ranges from 1 to 21600, and ρ ranges from 1800 to 6600.

Assume the camera produces perfect central projection, the relationship between the SPI and the original images can be described as Figure 1(b) shows, each pixel of the SPI can be determined by the lever-arm vector ($r_{C_i}^B$), and the corresponding vector ($r_p^{C_i}$) of the original image. The relationship between image point and the corresponding SPI point in the B-Frame is explained in Eq.(1), where $r_{p'}^B$ denotes SPI point coordinate defined in B-Frame; $r_p^{C_i}$ denotes Image point coordinate defined in C_i-Frame; μ denotes scale factor and $R_{C_i}^B$ denotes Rotation matrix from C_i-Frame to B-Frame. Besides, bilinear image resampling is applied to derive the color of a SPI point.

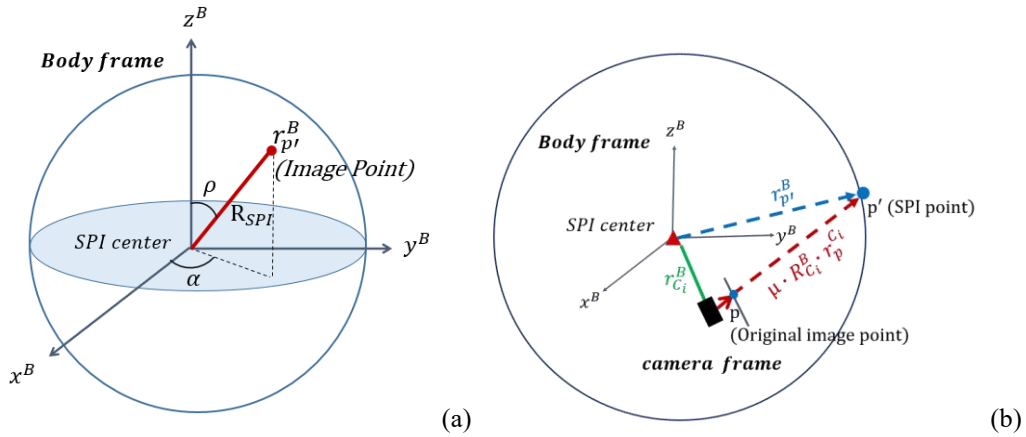

Figure 2 (a) The relationship between the B-Frame and the coordinate system of PPIMS SPI; (b) The geometric relationship between the SPI and original images.

$$r_{p'}^B = r_{C_i}^B + \mu \cdot R_{C_i}^B \cdot r_p^{C_i},\ i = 1 \sim 8 \tag{1}$$

3. IMAGE MATCHING FOR SPI INTERSECTION

3.1 Matching in the Object Space

With known EOPs of multiple SPIs, space intersection is applied to get the coordinate of object points which are observed on overlapped SPIs. After conjugate point are measured between overlapped SPIs, the coordinate of an object point can be solved by least square adjustment in ray intersection process.

Theoretically, if an object space plane is back projected to all original images which capture this plane, the projected planes derived from these overlapped images can form an identical projected image. Thus, if an assumed surface in object space is projected to the overlapped images and these projected surfaces lead to high correlations, which means they are similar to each other, these assumed surfaces is then considered to match the real surface. The concept is called matching in object space as Figure 3 shows. These assumed planes are back projected to images to acquire the

color of each pixel, and then these resampling images are used for matching.

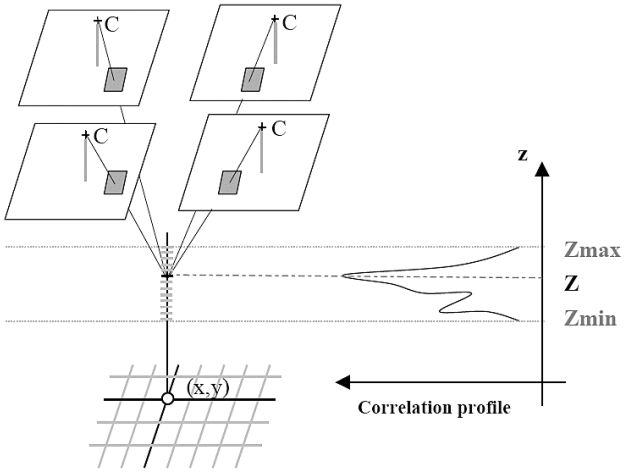

Figure 3 Multi-image Matching System from Object Space (Paparoditis et al., 2000).

The difference between matching in object space and image space is that object space matching is less suffered from the imaging geometry. With matching in object space, several surfaces need to be assumed, and the orientations of these assumed surfaces have to be close to the orientations of the real surfaces so that the two problems, scale variations and different field of view, can be solved.

3.2 Matching Index

Matching index is used to obtain the similarity between base image and match image. Two different matching index: Sum of Normalized Cross Correlation (SNCC) and Yet Another Reconstruction Dataprogram (YARD) are performed and compared in this study.

Normalized Cross Correlation (NCC) is widely used in computer vision field due to its robustness (Lewis, 1995; Einecke, 2010). It is an area-based matching method which uses the gray value of images for similarity measurement. NCC_k denotes the correlation coefficient between the base image in main station and each match image on other SPIs, which is used to check the similarity in between, higher correlation value means higher similarity of this image pair. The calculation method are explained in Eq. (2), where g_{ij} denotes the base image, and f_{ijk} denotes the match image f_{ij} in kth other SPIs. Sum of Normalized Cross Correlation (SNCC) is the average of NCC score, which checks the similarity between the base image and multiple SPIs, Eq. (3) explains the SNCC similarity index.

$$NCC_k = \frac{\sum\sum(f_{ijk}-\overline{f_k})(g_{ij}-\overline{g})}{\sqrt{\sum\sum(f_{ijk}-\overline{f_k})^2 \sum\sum(g_{ij}-\overline{g})^2}} \tag{2}$$

$$SNCC = \frac{1}{N}\sum NCC_k \tag{3}$$

The other matching index is called Yet Another Reconstruction Dataprogram (YARD) developed by Wiman (1998), using average image to calculate the correlation in object space to generate DSM automatically. Average image is formulated using the gray value average of all match images as Eq. (4) shows. In Wiman's study, there is no primary

image while we do have in this research. Thus the YARD is modified as Eq. (5) for our application.

$$Average\ \ image(f) = \frac{1}{N}\sum f_{ijk} \tag{4}$$

$$YARD = \frac{\sum\sum(f_{ij}-\overline{f})(g_{ij}-\overline{g})}{\sqrt{\sum\sum(f_{ij}-\overline{f})^2 \sum\sum(g_{ij}-\overline{g})^2}} \tag{5}$$

3.3 Implementation of Object Space Matching for SPIs

This section introduces the procedure of the proposed matching strategy for searching conjugate point with multiple SPIs. Object point coordinate can be calculated following the flowchart shown in Figure 4. Interest point should be measured in main SPI at the beginning, and a searching window with predefined size is defined, which is called base image. Similarity measurement is applied on base image in main SPI and match images in other searching SPIs.

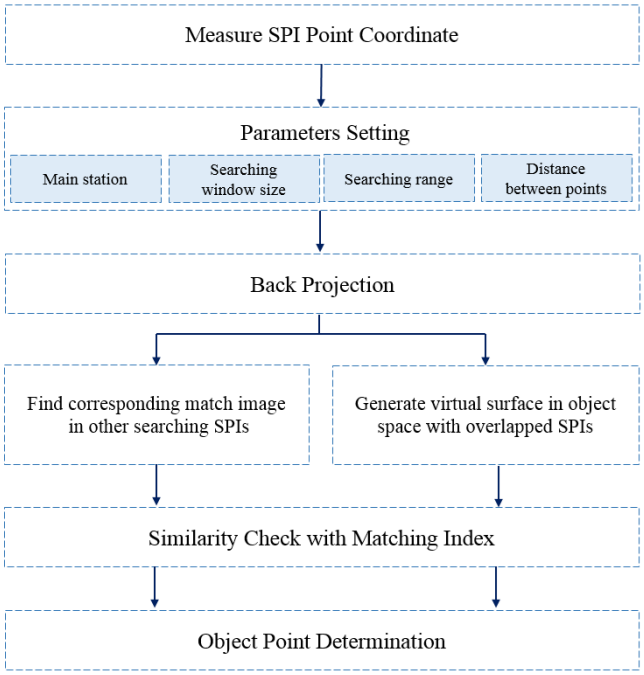

Figure 4 Flowchart for object space SPIs matching.

After the measurement of SPI point, back projection is applied. Choose a searching range along the light ray which pass through the SPI point and perspective center to generate possible points. For every single point within the searching range, project this point back to other SPIs to find the possible position of interest point p'', then the match image can be defined. Figure 5(a) illustrates the back projection concept between multiple SPIs.

Virtual surfaces are generated for scale and perspective adjustment. Once the interested point is chosen in main SPI, a series of assumed planes S_1 to S_n are created in object space along the vertical direction of base image in main SPI. Each plane is then back projected to other SPIs to get the match images using bilinear resampling. These projected images are therefore used for matching. Figure 5(b) shows the concept of virtual surface generation.

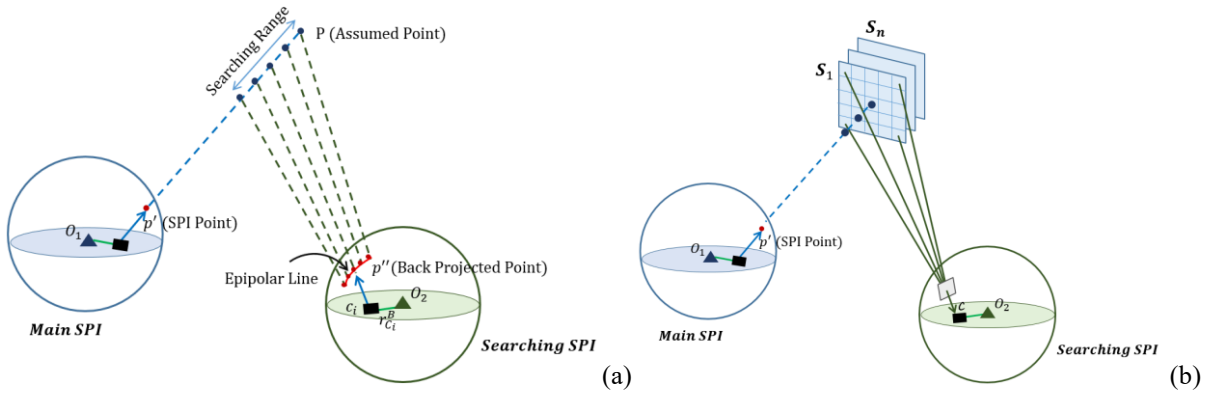

Figure 5 (a) Back projection of SPI; (b) Virtual surface generation in object space.

After finding corresponding match images which are formulated at the same assumed point, similarity measurement of each image group can be applied using same matching index, there is one similarity value in each assumed point. Then calculated similarity along the searching direction can be shown as similarity profile, which is used to detect the closest position of conjugate points. Figure 6 shows the concept of similarity profile. The position where the largest correlation value locates is regard as the conjugate point position.

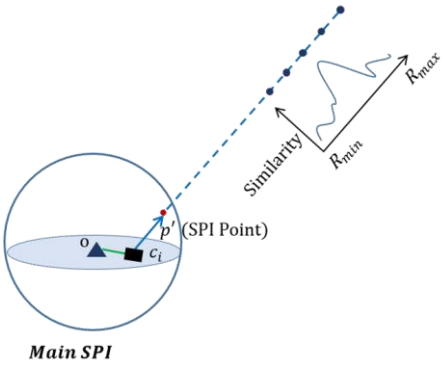

Figure 6 The concept of similarity profile.

4. Experiments

The indoor test field is set at the first floor of Dept. of Geomatics in NCKU. 5 SPIs are captured. 6 control points and 24 artificial targets on surrounding wall are selected as tie points which are used for EOPs calculation in multi-station network adjustment. Five captured SPIs and the position of tie points are shown in Figure 7.

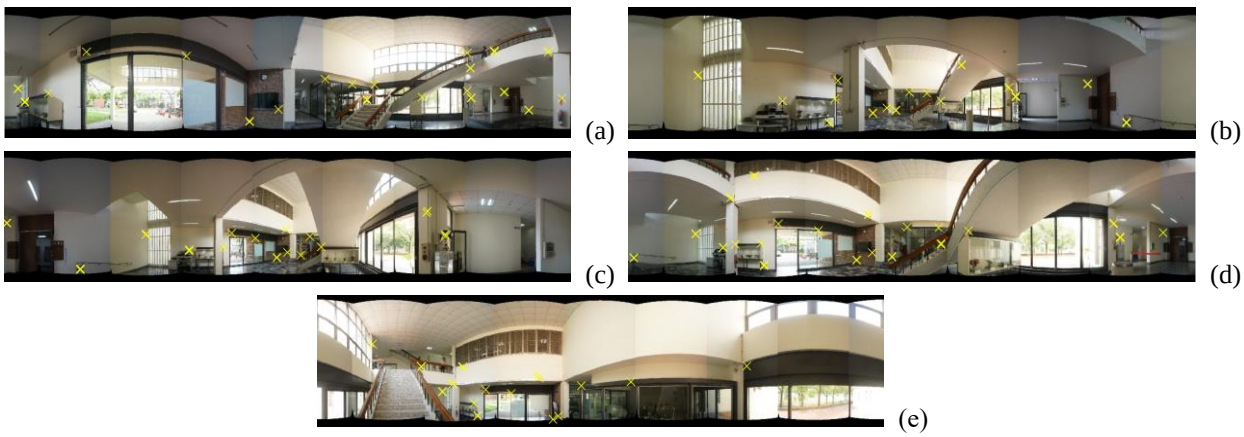

Figure 7 SPI of each image station and tie points distribution in indoor test field: (a) SPI2, (b) SPI 3 , (c) SPI 4, (d)

SPI 5, and (e) SPI 6.

Table 1 shows the standard deviations of the calculated EOPs of image stations. It seems that the precision of the coordinates of each station is better than ± 0.006m, and the precision of all rotation angles are better than $\pm 0.05°$.

Table 1 Standard deviations of image stations.

	$\hat{\sigma}_X$(m)	$\hat{\sigma}_Y$(m)	$\hat{\sigma}_Z$(m)	$\hat{\sigma}_\omega$(°)	$\hat{\sigma}_\varphi$(°)	$\hat{\sigma}_\kappa$(°)
SPI 2	±0.006	±0.005	±0.004	±0.043	±0.030	±0.029
SPI 3	±0.005	±0.005	±0.004	±0.042	±0.032	±0.028
SPI 4	±0.004	±0.004	±0.003	±0.042	±0.032	±0.027
SPI 5	±0.005	±0.004	±0.003	±0.042	±0.029	±0.025
SPI 6	±0.005	±0.004	±0.003	±0.050	±0.036	±0.032

After multi-station network adjustment, the EOPs of image stations are known, and space intersection can be applied. To validate the space intersection result, the coordinates of five target points are compared with the result of multi-station network adjustment. Table 2 shows the corresponding differences in each direction. The mean difference are all under 0.002 m, and the RMSD is better than ± 0.006 m in each direction. It reveals that the space intersection result is consistent to the multi-station adjustment result.

Table 2 Difference of target points.

	ΔX(m)	ΔY(m)	ΔZ(m)	Δd(m)
P1	0.003	-0.007	0.004	0.008
P4	0.000	-0.003	0.001	0.003
P8	-0.012	0.000	0.007	0.014
P27	0.001	0.000	0.000	0.001
P36	0.000	0.000	-0.001	0.001
Mean	-0.002	-0.002	0.002	
RMSD	±0.006	±0.003	±0.004	

Figure 8 shows the similarity profiles of selected targets. According to profile curves of Case 1 and Case 2, it seems that the curves do not show the peak clearly, and where the highest similarity values locate do not indicate the correct point position. Take point ID 1 for example, the highest similarity of these two cases locate are more than 20 cm away from the central position. As for the corresponding profile curves of Case 3 and Case 4, all targets show the peak very clearly at the central position. With these test results, it may be concluded that matching with object space images can perform higher similarity than using original images. Table 3 shows the maximum similarity value of test targets in each test case. Comparing the corresponding cases of same matching index, most similarity value using object space images are larger than using original images. Applying original images for matching, the average similarity using SNCC and YARD index are 0.380 and 0.574, and the values enhance to 0.573 and 0.696 with object space images. It reveals that using object space images for matching may reach better performance.

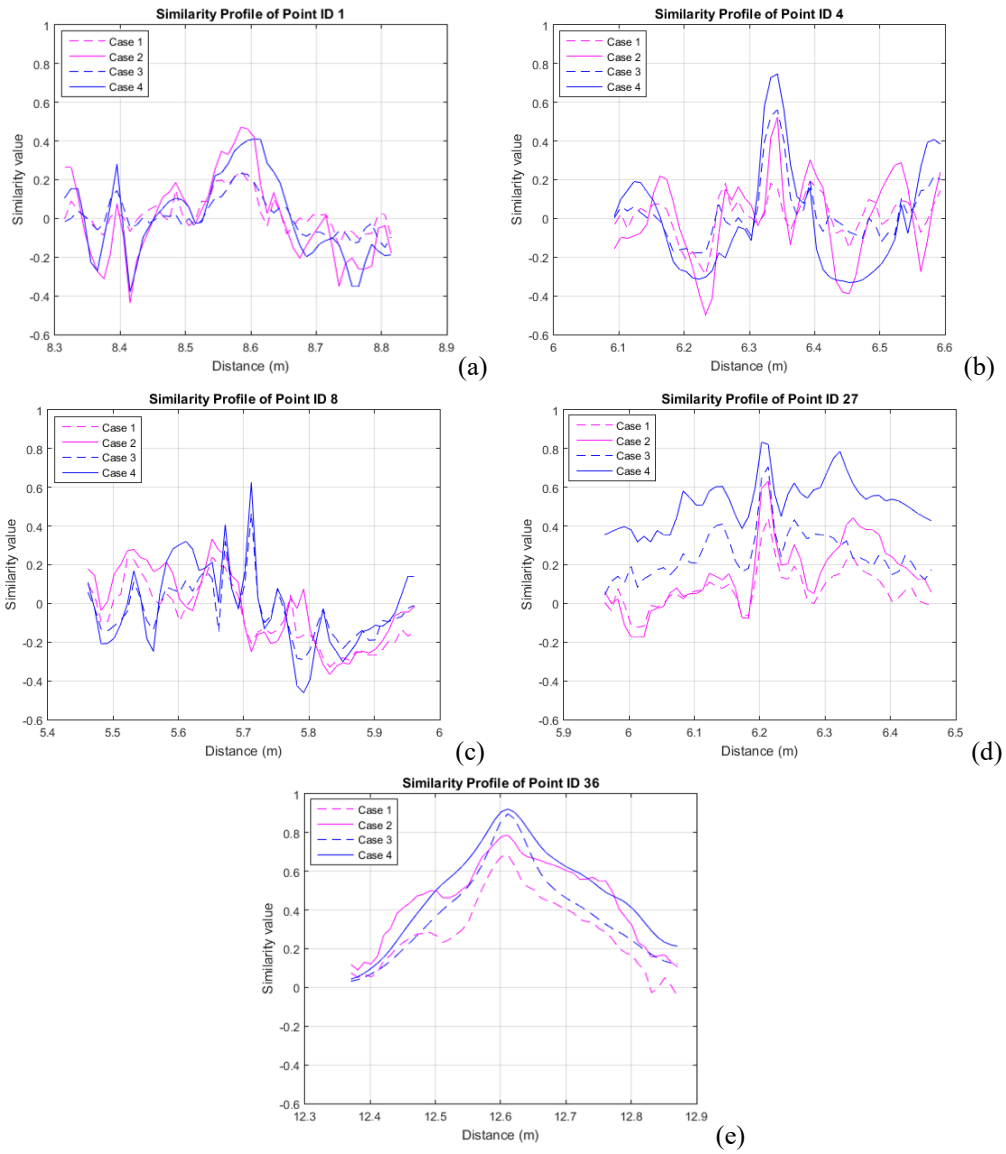

Figure 8 Similarity profiles: (a)Point ID 1, (b)Point ID 4, (c)Point ID 8, (d)Point ID 27, and (e)Point ID 36.

Table 3 Maximum similarity of test targets.

	Case 1	**Case 2**	**Case 3**	**Case 4**
Matching Index	SNCC	YARD	SNCC	YARD
Match Image Type	Image Space	Image Space	Object Space	Object Space
P1	0.248	0.472	0.232	0.411
P4	0.193	0.523	0.563	0.747
P8	0.242	0.333	0.465	0.624
P27	0.533	0.757	0.706	0.777
P36	0.684	0.787	0.897	0.922
Average	0.380	0.574	0.573	0.696

At last, the image matching results of five test targets will be shown and analyzed. Table 4 and Table 5 show the differences of check points in each direction with the cases using original images and object space images results

respectively. The results are compared to the results of multi-station network adjustment. Also, the mean difference (Mean.) and the RMSD are calculated.

In Table 4, the maximum mean difference is 2.2 cm in the Y direction of Case 1, and the maximum value of RMSD is ±3.3 cm, which also appears in the same direction. In Table 5, all of the mean difference are under 0.5 cm in each direction, and the RMSD value are under 1 cm. From the searching results, it reveals that the object point position can be calculated precisely with object space image matching. Also, the mean difference and the RMSD of Case 2 and Case 4 are smaller than the result of Case 1 and Case 3. It reveals that using YARD index for image matching may provide the result more reliable than using SNCC index.

Table 4 Check points comparison (Part 1).

	Case 1			**Case 2**		
	ΔX (m)	ΔY (m)	ΔZ (m)	ΔX (m)	ΔY (m)	ΔZ (m)
P1	-0.007	0.002	0.006	-0.007	0.002	0.006
P4	-0.026	0.043	0.007	-0.005	-0.002	-0.003
P8	-0.012	0.060	-0.006	-0.012	0.060	-0.006
P27	0.000	0.000	0.001	0.000	0.000	0.001
P36	0.011	0.003	-0.004	0.011	0.003	-0.004
Mean	-0.007	0.022	0.001	-0.003	0.013	-0.001
RMSD	±0.014	±0.033	±0.005	±0.008	±0.027	±0.005

Table 5 Check points comparison (Part 2).

	Case 3			**Case 4**		
	ΔX (m)	ΔY (m)	ΔZ (m)	ΔX (m)	ΔY (m)	ΔZ (m)
P1	-0.007	0.002	0.006	-0.015	-0.017	0.010
P4	-0.005	-0.002	-0.003	-0.005	-0.002	-0.003
P8	-0.013	0.001	0.004	-0.013	0.001	0.004
P27	0.000	0.000	0.001	0.000	0.000	0.001
P36	0.011	0.003	-0.004	0.011	0.003	-0.004
Mean	-0.003	0.001	0.001	-0.004	-0.003	0.002
RMSD	±0.009	±0.002	±0.004	±0.010	±0.008	±0.005

Compare to the result of preliminary test, the point searching results are better than the result in the test field. In preliminary test, the standard deviation of estimated image positions is about 1 mm, and that of estimated rotation angles, the precision are better than 0.05 degrees. The corresponding values in the test field are 6 mm and 0.5 degrees. From these results, it may be concluded that the accuracy of back projection and image matching is influenced by the standard deviations of image station EOPs.

5. CONCLUSIONS

In this study, a method for photogrammetric mapping is developed based on SPIs. Space intersection can be performed by SPI point measurement while the E.O. parameters of image stations are known. An indoor test field is done in this study to validate the idea, and the space intersection result is compared to the result of multi-station network adjustment in solving image station EOPs. The RMSD value of target points are ($\pm$0.006m, $\pm$0.003m, $\pm$0.004m) in three directions, which validates the availability of measurement application using PPIMS. On the other hand, a matching strategy for conjugate point searching with PPIMS SPIs is proposed. In the preliminary image matching test, the similarity profiles of object space images show higher searching accuracy. For the practical experiment, the RMSD of searching points with original images are ($\pm$0.014m, $\pm$0.033m, $\pm$0.005m) in three directions with SNCC index, and ($\pm$0.008m, $\pm$0.027m, $\pm$0.005m) with YARD index. With object space matching, the corresponding results are ($\pm$0.009m, $\pm$0.002m, $\pm$0.004m) with SNCC index, and ($\pm$0.010m, $\pm$0.008m, $\pm$0.005m) with YARD index. Again, the results show better positioning accuracy with object space matching. From these experimental results, the idea of space intersection with PPIMS SPIs can be achieved. Using SPIs for photogrammetric triangulation and mapping is feasible. Also, the proposed matching strategy is validated, conjugate points detection and point coordinate determination can be achieved by object space matching with multiple SPIs. So far, the point searching accuracy is in cm level with reliable image station EOPs. The problem of scale variations and different FOV which causes problem in matching with original images can be improved by object space image matching.

6. REFERENCES

Einecke, N. and J. Eggert, 2010. A Two-Stage Correlation Method for Stereoscopic Depth Estimation. Digital Image Computing: Techniques and Applications 2010 IEEE, pp. 227-233.

Gruen, A.W., 1985. Adaptive Least Squares Correlation: A Powerful Image Matching Technique. Photogrammetry, Remote Sensing and Cartography 14(3):175-187.

Lewis, J. P. 1995. Fast Template Matching. Vision Interface, pp. 120-123.

Lin, K.Y., 2014. Bundle Adjustment of Multi-station Spherical Panorama Images with GPS Positioning. Master's Thesis. Department of Geomatics. National Cheng Kung University, Taiwan.

Paparoditis, N., C. Thom, and H. Jibrini, 2000. Surface Reconstruction in Urban Areas from Multiple Views of Aerial Digital Frame Cameras. International Archives of Photogrammetry and Remote Sensing, Vol.33, Supplement B3, pp.43-50.

Wang, P.C., 2012. System Calibration of a Portable Panoramic Image Mapping System (PPIMS). Master's Thesis. Department of Geomatics, National Cheng Kung University.

Tsai, P.C., 2012. Bundle Adjustment and Application of a Portable Panoramic Image Mapping System (PPIMS). Master's Thesis. Department of Geomatics. National Cheng Kung University, Taiwan.